

# Mueller Navelet jets at LHC: A clean test of QCD resummation effects at high energy?

Bertrand Ducloué

Laboratoire de Physique Théorique d'Orsay

Marseille, April 25th 2013

in collaboration with

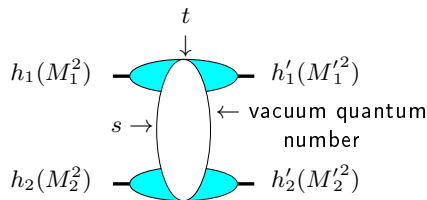
L. Szymanowski (NCBJ, Warsaw), S. Wallon (UPMC & LPT Orsay)

D. Colferai; F. Schwennsen, L. Szymanowski, S. Wallon, JHEP 1012:026 (2010) 1-72  
[arXiv:1002.1365]

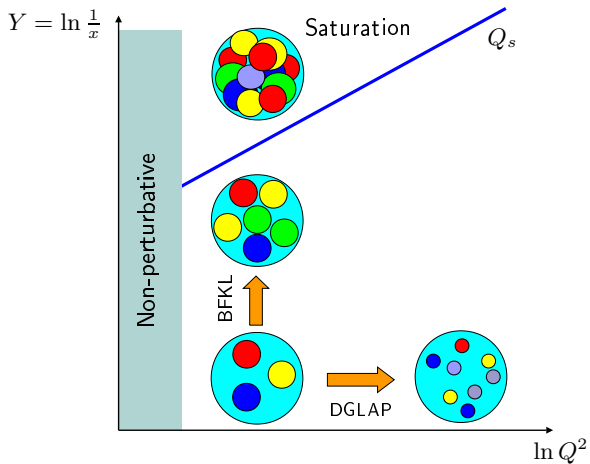
B.D., L. Szymanowski, S. Wallon, arXiv:1208.6111

B.D., L. Szymanowski, S. Wallon, arXiv:1302.7012 (to appear in JHEP)

- One of the important longstanding theoretical questions raised by QCD is its behaviour in the perturbative **Regge** limit  $s \gg -t$
- Based on theoretical grounds, one should identify and test suitable observables in order to test this peculiar dynamics



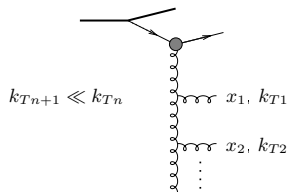
hard scales:  $M_1^2, M_2^2 \gg \Lambda_{QCD}^2$  or  $M_1'^2, M_2'^2 \gg \Lambda_{QCD}^2$  or  $t \gg \Lambda_{QCD}^2$   
 where the  $t$ -channel exchanged state is the so-called **hard Pomeron**



Small values of  $\alpha_S$  (perturbation theory applies due to hard scales) can be compensated by large logarithmic enhancements.

⇒ resummation of  $\sum_n (\alpha_S \ln A)^n$  series

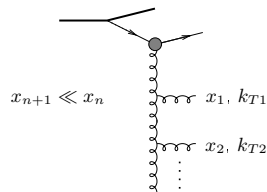
DGLAP



strong ordering in  $k_T$

$$\sum (\alpha_S \ln \frac{Q^2}{\mu^2})^n$$

BFKL



strong ordering in  $x$

$$\sum (\alpha_S \ln \frac{s}{s_0})^n$$

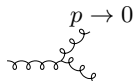
When  $\sqrt{s}$  becomes very large, it is expected that a BFKL description is needed to get accurate predictions

## What kind of observables?

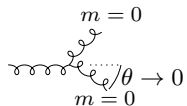
- perturbation theory should be applicable:

selecting external or internal probes with transverse sizes  $\ll 1/\Lambda_{QCD}$  or by choosing large  $t$  in order to provide the hard scale

- governed by the *soft* perturbative dynamics of QCD



and *not* by its *collinear* dynamics



$\Rightarrow$  select semi-hard processes with  $s \gg p_{T i}^2 \gg \Lambda_{QCD}^2$  where  $p_{T i}^2$  are typical transverse scale, **all of the same order**

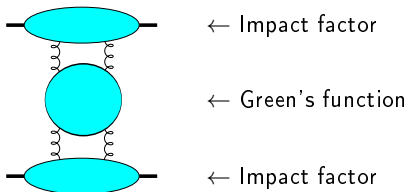
## QCD in the perturbative Regge limit

The amplitude can be written as:

$$\mathcal{A} = \underbrace{\text{Diagram 1}}_{\sim s} + \left( \underbrace{\text{Diagram 2}}_{\sim s} + \underbrace{\text{Diagram 3}}_{\sim s} + \dots \right) + \left( \underbrace{\text{Diagram 4}}_{\sim s} + \dots \right) + \dots$$

Diagram 1: Two light blue ovals (impact factors) connected by two vertical wavy lines (gluons).  
 Diagram 2: Two light blue ovals connected by two vertical wavy lines, with a horizontal wavy line connecting the two vertical lines.  
 Diagram 3: Two light blue ovals connected by two vertical wavy lines, with a circular loop of wavy lines connecting the two vertical lines.  
 Diagram 4: Two light blue ovals connected by two vertical wavy lines, with three horizontal wavy lines connecting the two vertical lines.

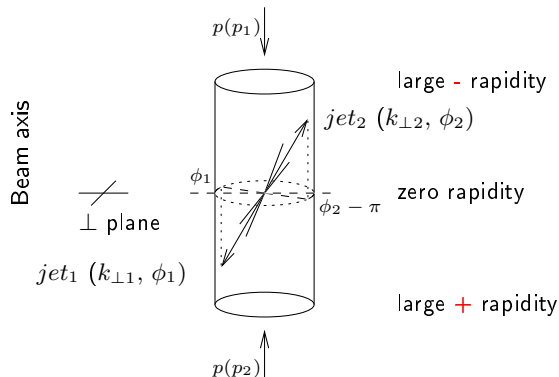
this can be put in the following form :



- Higher order corrections to BFKL kernel are known at NLL order (Lipatov Fadin; Camici, Ciafaloni), now for arbitrary impact parameter  $\alpha_S \sum_n (\alpha_S \ln s)^n$  resummation
- impact factors are known in some cases at NLL
  - $\gamma^* \rightarrow \gamma^*$  at  $t = 0$  (Bartels, Colferai, Gieseke, Kyrieleis, Qiao; Balitski, Chirilli)
  - forward jet production (Bartels, Colferai, Vacca)
  - inclusive production of a pair of hadrons separated by a large interval of rapidity (Ivanov, Papa)
  - $\gamma_L^* \rightarrow \rho_L$  in the forward limit (Ivanov, Kotsky, Papa)

## Mueller-Navelet jets

- Consider two jets (hadrons flying within a narrow cone) **separated by a large rapidity**, i.e. each of them almost fly in the direction of the hadron “close” to it, and with very similar transverse momenta
- in a pure LO collinear treatment, these two jets should be emitted **back to back** at leading order:  $\Delta\phi - \pi = 0$  ( $\Delta\phi = \phi_1 - \phi_2 =$  relative azimuthal angle) and  $k_{\perp 1} = k_{\perp 2}$ . There is no phase space for (untagged) emission between them





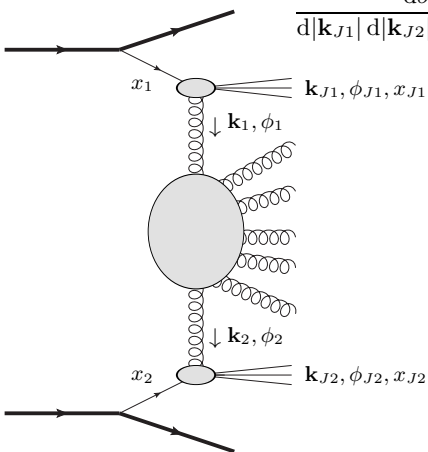
$k_T$ -factorized differential cross-section

$$\frac{d\sigma}{d|\mathbf{k}_{J1}| d|\mathbf{k}_{J2}| dy_{J1} dy_{J2}} = \int d\phi_{J1} d\phi_{J2} \int d^2\mathbf{k}_1 d^2\mathbf{k}_2$$

$$\times \Phi(\mathbf{k}_{J1}, x_{J1}, -\mathbf{k}_1)$$

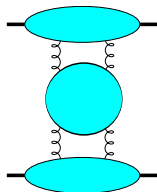
$$\times G(\mathbf{k}_1, \mathbf{k}_2, \hat{s})$$

$$\times \Phi(\mathbf{k}_{J2}, x_{J2}, \mathbf{k}_2)$$



$$\text{with } \Phi(\mathbf{k}_{J2}, x_{J2}, \mathbf{k}_2) = \int dx_2 f(x_2) V(\mathbf{k}_2, x_2) \quad f \equiv \text{PDF} \quad x_J = \frac{|\mathbf{k}_J|}{\sqrt{s}} e^{y_J}$$

- in LL BFKL ( $\sim \sum (\alpha_s \ln s)^n$ ), the emission between these jets leads to a **strong decorrelation** between the jets, incompatible with  $p\bar{p}$  Tevatron collider data
- up to recently, the subseries  $\alpha_s \sum (\alpha_s \ln s)^n$  NLL was included only in the Green's function, and not inside the jet vertices  
Sabio Vera, Schwennsen  
Marquet, Royon
- the importance of these corrections was not known



## Results for a symmetric configuration

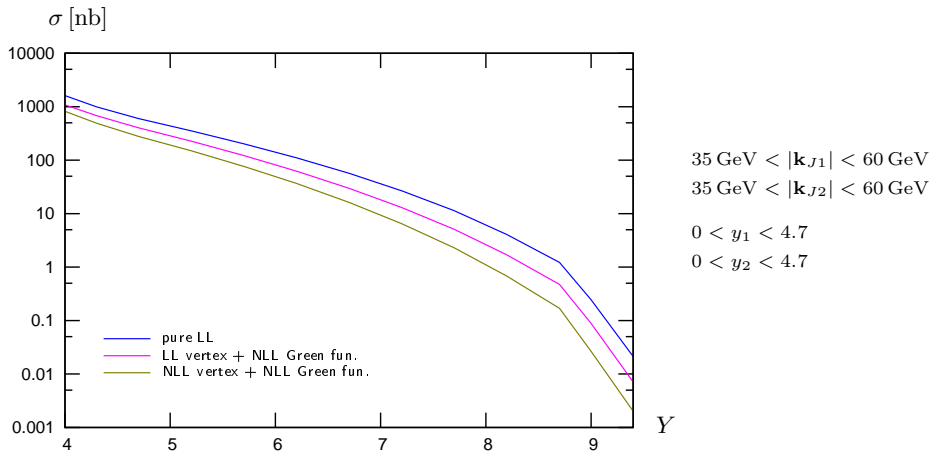
In the following we show results for

- $35 \text{ GeV} < |\mathbf{k}_{J1}|, |\mathbf{k}_{J2}| < 60 \text{ GeV}$
- $0 < y_1, y_2 < 4.7$

These cuts allow us to compare our results with preliminary results from CMS (see talk by [A. Knutsson](#)).

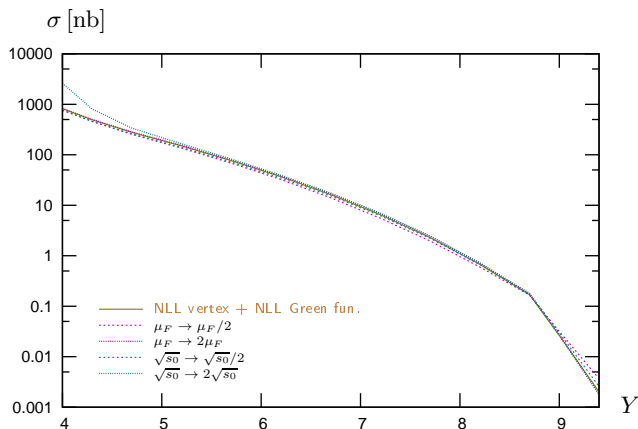
note: unlike experiments we have to set an upper cut on  $|\mathbf{k}_{J1}|$  and  $|\mathbf{k}_{J2}|$ . We have checked that varying this cut doesn't modify our results significantly.

## Cross-section



The effect due to NLL corrections to the jet vertex is of the same order of magnitude as the effect due to NLL corrections to the Green's function.

Cross-section: stability with respect to  $s_0$  and  $\mu_R = \mu_F$  changes



$35 \text{ GeV} < |\mathbf{k}_{J1}| < 60 \text{ GeV}$

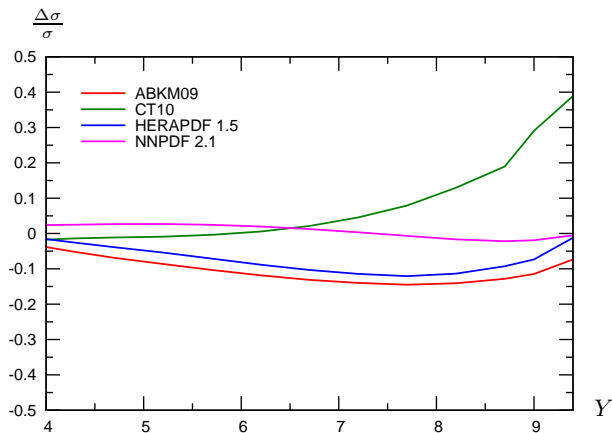
$35 \text{ GeV} < |\mathbf{k}_{J2}| < 60 \text{ GeV}$

$0 < y_1 < 4.7$

$0 < y_2 < 4.7$

Our result is rather stable w.r.t  $s_0$  and  $\mu$  choices.

## Relative variation of the cross section when using other PDF sets than MSTW 2008

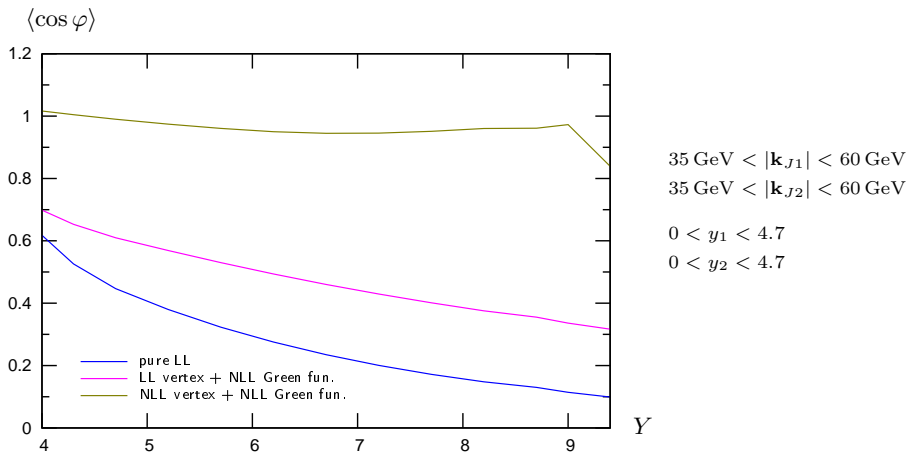


$$35 \text{ GeV} < |\mathbf{k}_{J1}| < 60 \text{ GeV}$$

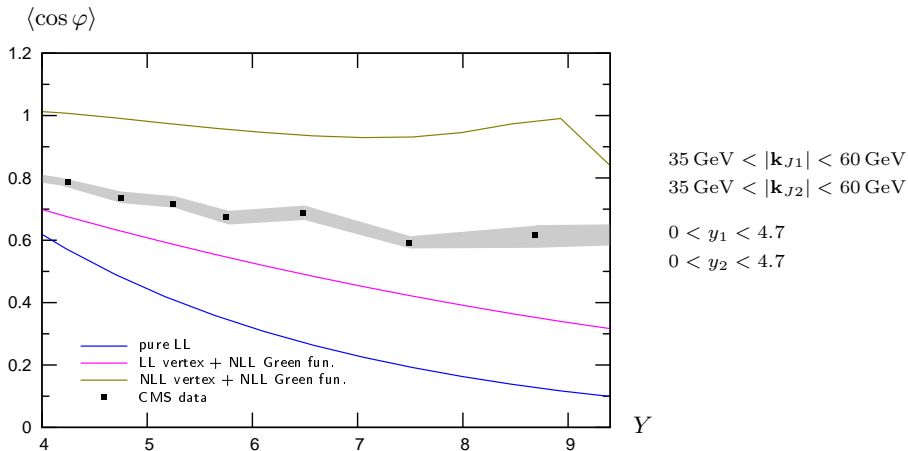
$$35 \text{ GeV} < |\mathbf{k}_{J2}| < 60 \text{ GeV}$$

$$0 < y_1 < 4.7$$

$$0 < y_2 < 4.7$$

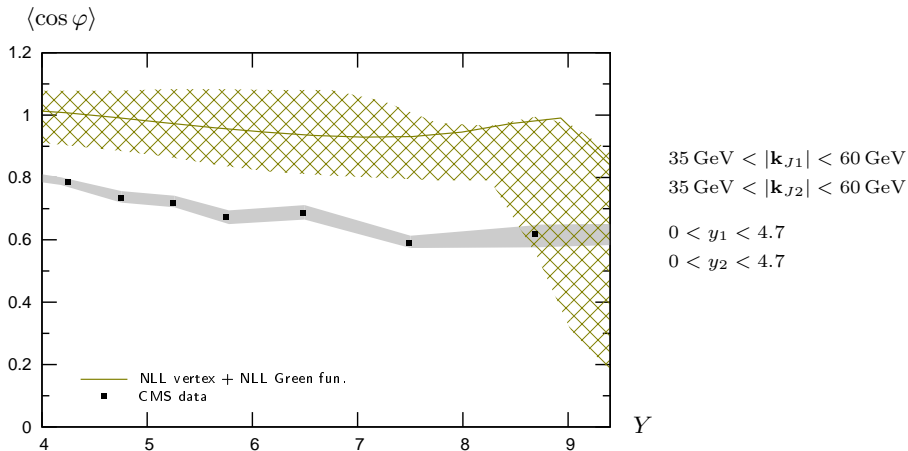
Azimuthal correlation  $\langle \cos \varphi \rangle$ 

- The effect of NLL corrections to the jet vertex is very important
- At full NLL accuracy,  $\langle \cos \varphi \rangle$  is very flat in  $Y$  and very close to 1.

Azimuthal correlation  $\langle \cos \varphi \rangle$ 

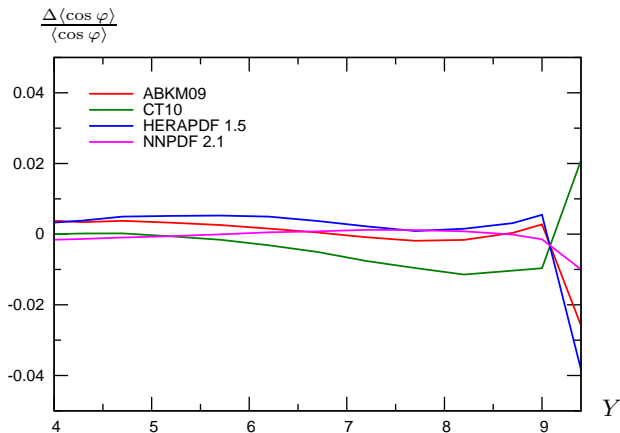
- None of the BFKL computations describe the data very well



Azimuthal correlation  $\langle \cos \varphi \rangle$ 

- None of the BFKL computations describe the data very well
- The result at NLL is still rather dependent on the choice of  $s_0$  and  $\mu_R = \mu_F$

Relative variation of  $\langle \cos \varphi \rangle$  when using other PDF sets than MSTW 2008

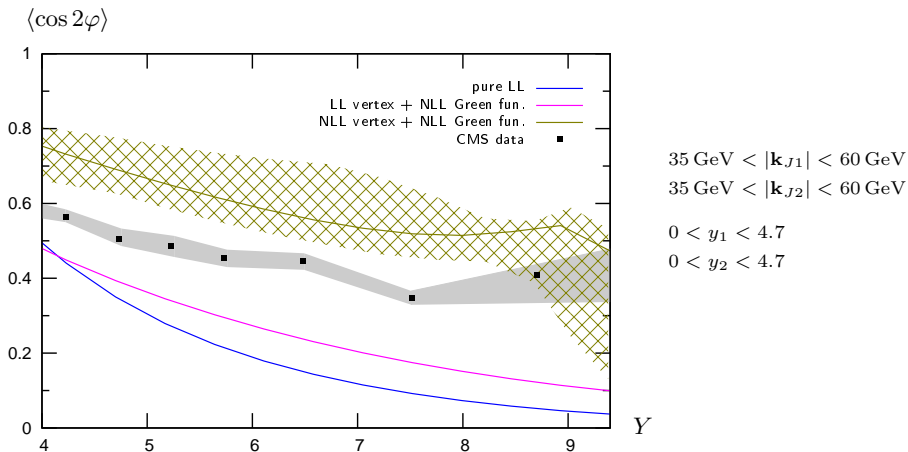


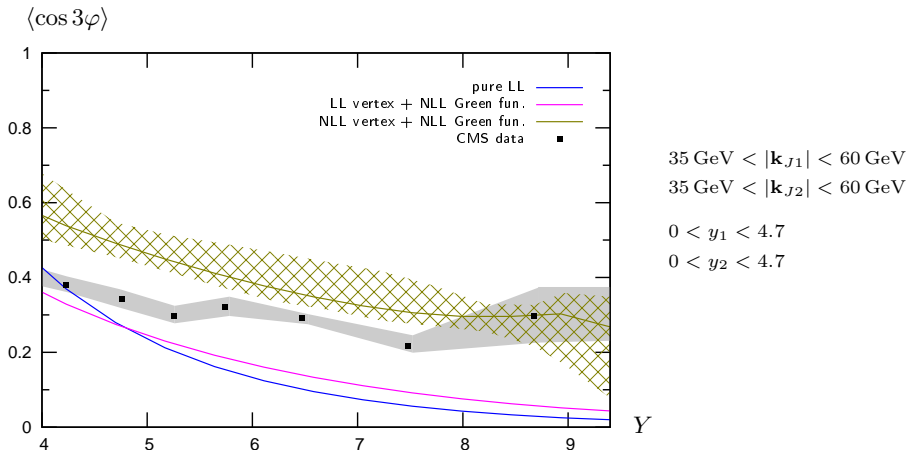
$35 \text{ GeV} < |\mathbf{k}_{J1}| < 60 \text{ GeV}$

$35 \text{ GeV} < |\mathbf{k}_{J2}| < 60 \text{ GeV}$

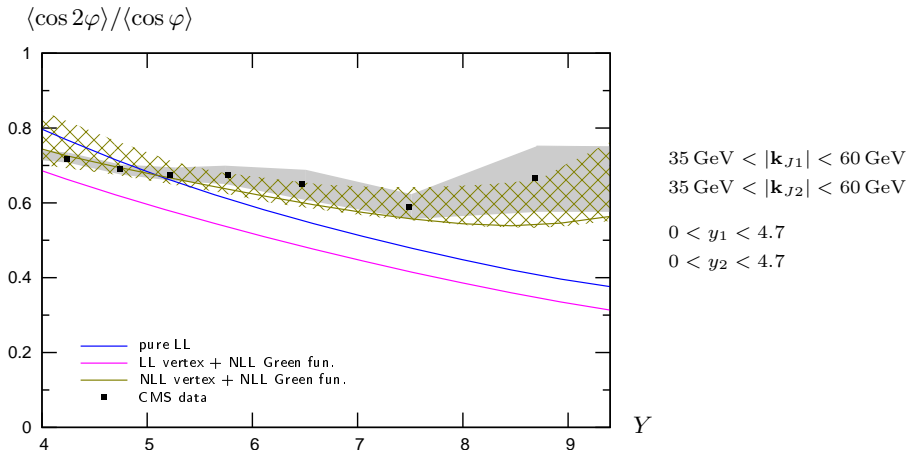
$0 < y_1 < 4.7$

$0 < y_2 < 4.7$

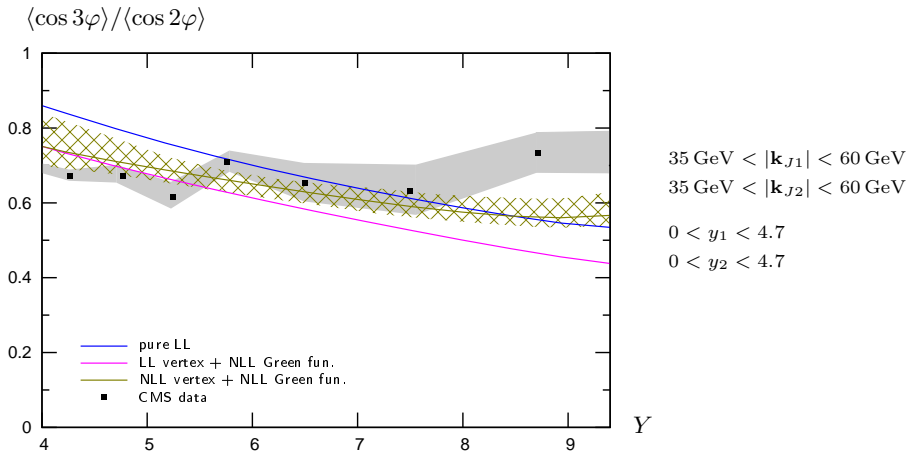
Azimuthal correlation  $\langle \cos 2\varphi \rangle$ 

Azimuthal correlation  $\langle \cos 3\varphi \rangle$ 

Taking into account the uncertainty associated with the choice of the scales, NLL BFKL is quite close to the data for  $Y \gtrsim 6$ .

Azimuthal correlation  $\langle \cos 2\varphi \rangle / \langle \cos \varphi \rangle$ 

The observable  $\langle \cos 2\varphi \rangle / \langle \cos \varphi \rangle$  is described reasonably well by NLL BFKL.

Azimuthal correlation  $\langle \cos 3\varphi \rangle / \langle \cos 2\varphi \rangle$ 

The 3 different BFKL computations for  $\langle \cos 3\varphi \rangle / \langle \cos 2\varphi \rangle$  are quite close to each other

- We have deepened our complete NLL analysis of **Mueller-Navelet** jets
- **First comparison to data** taken at LHC for the azimuthal correlations
- The effect of NLL corrections to the vertices is dramatic, similar to the NLL Green's function corrections
- For the **cross-section**:  
makes prediction more stable with respect to variation of scales  $\mu$  and  $s_0$
- Surprisingly small **decorrelation** effect: NLL BFKL underestimates the decorrelation
- $\langle \cos \varphi \rangle$ ,  $\langle \cos 2\varphi \rangle$  and  $\langle \cos 3\varphi \rangle$  are still rather dependent on the choice of the scales  
Ratios of these quantities are more stable
- For  $\langle \cos 2\varphi \rangle / \langle \cos \varphi \rangle$ , data is quite well described by NLL BFKL
- **Mueller Navelet jets** provide much more complicate observables than expected

Backup



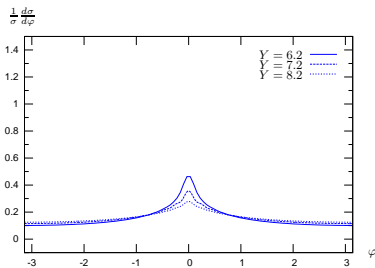
## Azimuthal distribution

Computing  $\langle \cos(n\phi) \rangle$  up to large values of  $n$  gives access to the angular distribution

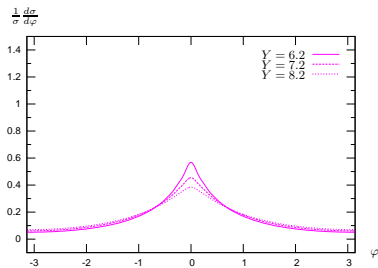
$$\frac{1}{\sigma} \frac{d\sigma}{d\phi} = \frac{1}{2\pi} \left\{ 1 + 2 \sum_{n=1}^{\infty} \cos(n\phi) \langle \cos(n\phi) \rangle \right\}$$

This is a quantity accessible at experiments like **ATLAS** and **CMS**

## Azimuthal distribution



pure LL



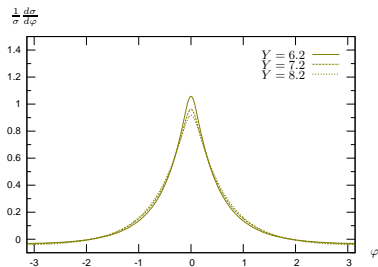
LL vertices + NLL Green's fun.

$$35 \text{ GeV} < |\mathbf{k}_{J1}| < 60 \text{ GeV}$$

$$35 \text{ GeV} < |\mathbf{k}_{J2}| < 60 \text{ GeV}$$

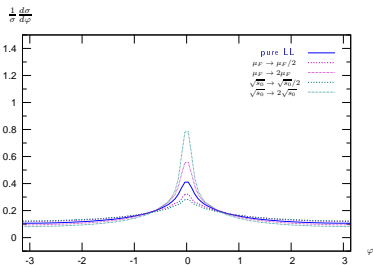
$$0 < y_1 < 4.7$$

$$0 < y_2 < 4.7$$

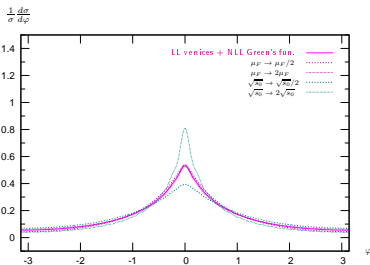


NLL vert. + NLL Green's fun.

## Azimuthal distribution: stability with respect to $s_0$ and $\mu_R = \mu_F$



pure LL



LL vertices + NLL Green's fun.

$$35 \text{ GeV} < |\mathbf{k}_{J1}| < 60 \text{ GeV}$$

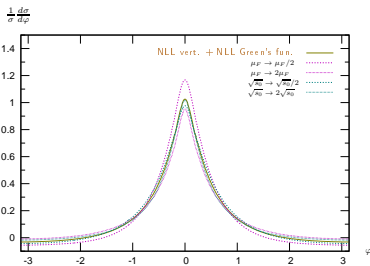
$$35 \text{ GeV} < |\mathbf{k}_{J2}| < 60 \text{ GeV}$$

$$0 < y_1 < 4.7$$

$$0 < y_2 < 4.7$$

integrating on the bin:

$$6 < Y = y_1 + y_2 < 9.4$$



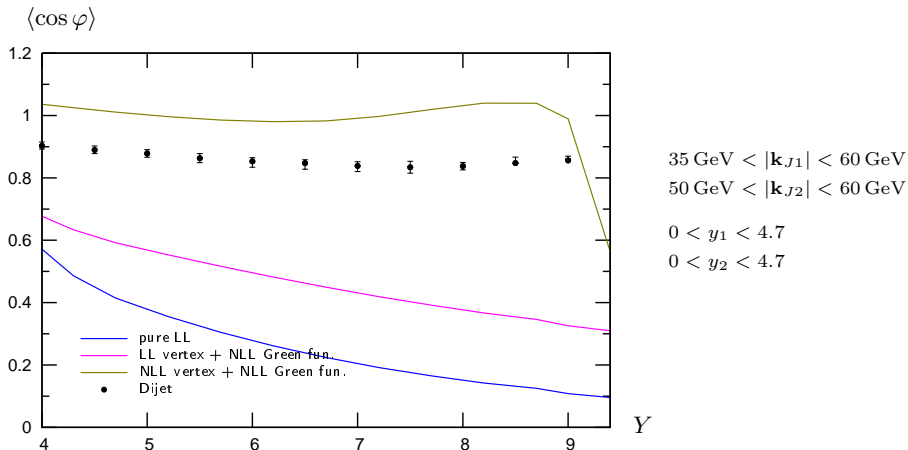
NLL vert. + NLL Green's fun.

## Results for an asymmetric configuration

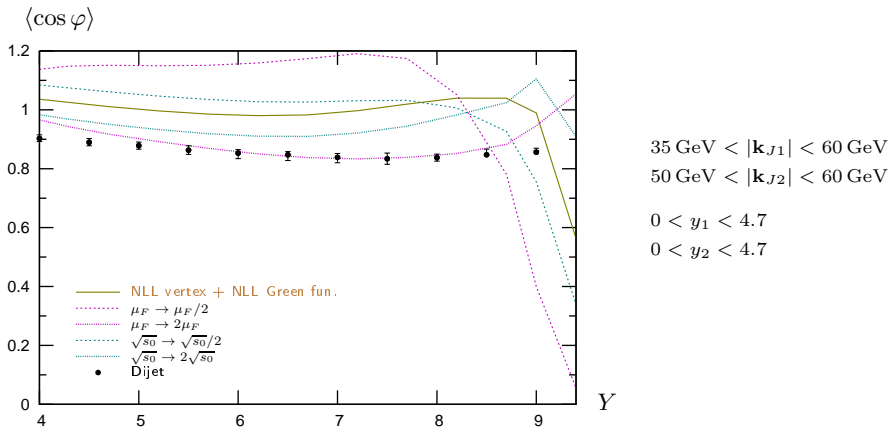
In this section we choose the cuts as

- $35 \text{ GeV} < |\mathbf{k}_{J1}| < 60 \text{ GeV}$
- $50 \text{ GeV} < |\mathbf{k}_{J2}| < 60 \text{ GeV}$
- $0 < y_1, y_2 < 4.7$

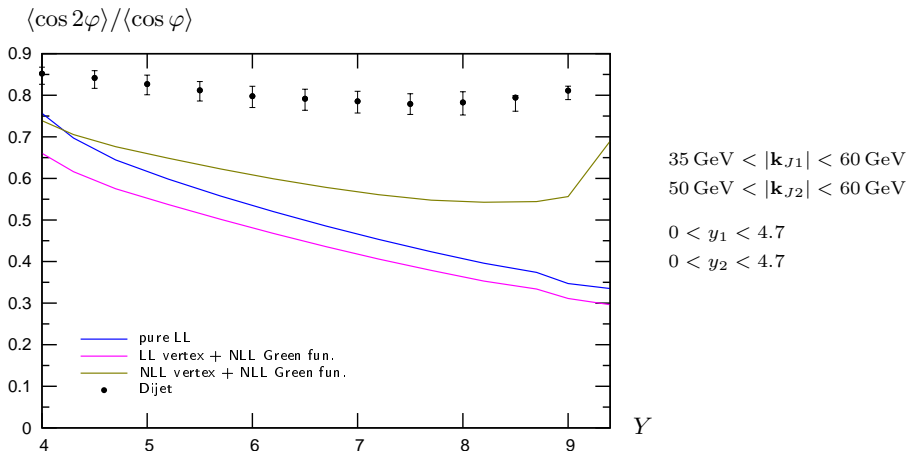
Such an asymmetric configuration allows us to do a comparison with results obtained by fixed order calculation.

Azimuthal correlation  $\langle \cos \varphi \rangle$ : fixed order NLO versus NLL BFKL

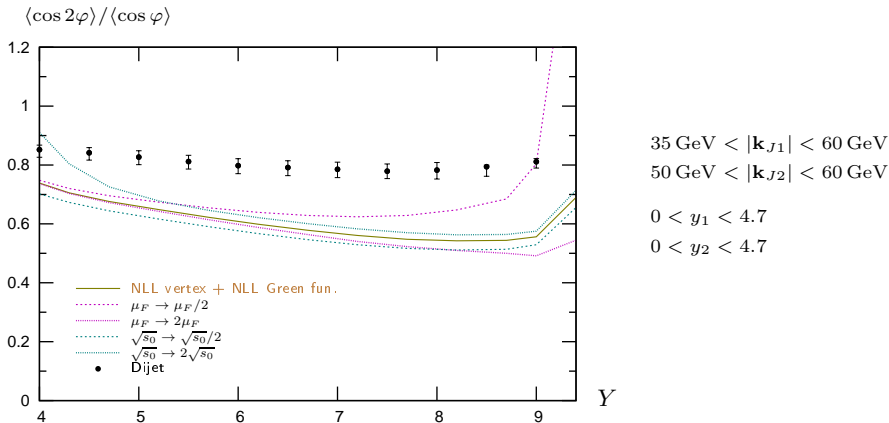
dots = based on the fixed order NLO parton generator *Dijet* (thanks to M. Fontannaz)

Azimuthal correlation:  $\langle \cos \varphi \rangle$ 

- Putting (almost) the same scale, exactly the same cuts, we get a difference between fixed order NLO and NLL BFKL for  $4.5 < Y < 8.5$
- This difference is washed-out because of  $s_0$  and  $\mu$  dependency

Azimuthal correlation  $\langle \cos 2\varphi \rangle / \langle \cos \varphi \rangle$ : fixed order NLO versus NLL BFKL

dots = based on the fixed order NLO parton generator *Dijet* (thanks to M. Fontannaz)

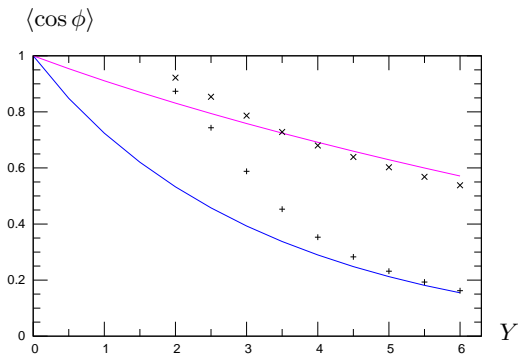
Azimuthal correlation:  $\langle \cos 2\varphi \rangle / \langle \cos \varphi \rangle$ 

- fixed order NLO and NLL BFKL differ significantly for  $4.5 < Y < 8$
- This result is rather stable w.r.t  $s_0$  and  $\mu$  choices.



## Comparison in the simplified NLL Green's function + LL jet vertices scenario

- The integration  $\int_{k_{Jmin}}^{\infty} dk_J$  can be performed analytically
- A comparison with the numerical integration based on code provides a good test of stability, valid for large  $Y$



blue: LL

magenta: NLL Green's function + LL jet vertices scenario Sabio Vera, Schwennsen

×: numerical  $dk_J$  integration

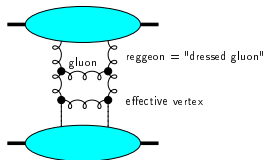
$k_{J1} > 20$  GeV and  $k_{J2} > 50$  GeV

## QCD in the perturbative Regge limit

- Small values of  $\alpha_S$  (perturbation theory applies due to hard scales) can be compensated by large  $\ln s$  enhancements.  $\Rightarrow$  resummation of  $\sum_n (\alpha_S \ln s)^n$  series (Balitski, Fadin, Kuraev, Lipatov)

$$\mathcal{A} = \underbrace{\text{Diagram 1}}_{\sim s} + \left( \underbrace{\text{Diagram 2}}_{\sim s(\alpha_S \ln s)} + \underbrace{\text{Diagram 3}}_{\sim s(\alpha_S \ln s)} + \dots \right) + \left( \underbrace{\text{Diagram 4}}_{\sim s(\alpha_S \ln s)^2} + \dots \right) + \dots$$

- this results in the effective BFKL ladder

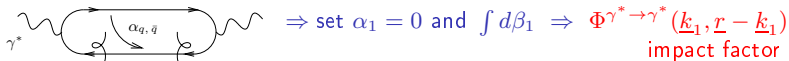


$$\Rightarrow \sigma_{tot}^{h_1 h_2 \rightarrow anything} = \frac{1}{s} \text{Im} \mathcal{A} \sim s^{\alpha_{\mathbb{P}}(0) - 1}$$

with  $\alpha_{\mathbb{P}}(0) - 1 = C \alpha_S$  ( $C > 0$ )    Leading Log Pomeron  
Balitsky, Fadin, Kuraev, Lipatov

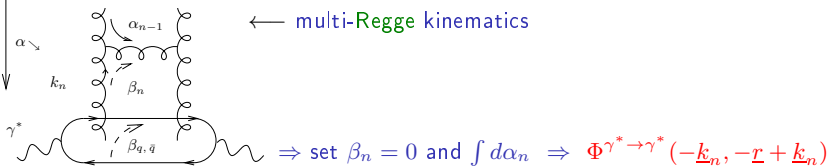
# Opening the boxes: Impact representation $\gamma^* \gamma^* \rightarrow \gamma^* \gamma^*$ as an example

- Sudakov decomposition:  $k_i = \alpha_i p_1 + \beta_i p_2 + k_{\perp i}$  ( $p_1^2 = p_2^2 = 0$ ,  $2p_1 \cdot p_2 = s$ )
- write 
$$d^4 k_i = \frac{s}{2} d\alpha_i d\beta_i d^2 k_{\perp i} \quad (\underline{k} = \text{Eucl.} \leftrightarrow k_{\perp} = \text{Mink.})$$
- $t$ -channel gluons have non-sense polarizations at large  $s$ :  $\epsilon_{NS}^{up/down} = \frac{2}{s} p_{2/1}$



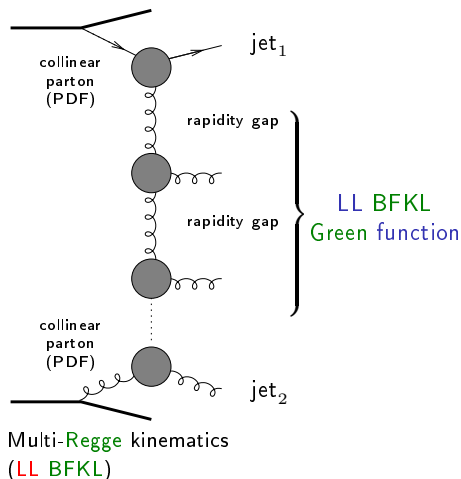
$$\mathcal{M} = \frac{is}{(2\pi)^2} \int \frac{d^2 \underline{k}}{\underline{k}^2} \Phi^{up}(\underline{k}, \underline{r} - \underline{k}) \int \frac{d^2 \underline{k}'}{\underline{k}'^2} \Phi^{down}(-\underline{k}', -\underline{r} + \underline{k}') \\ \times \int_{\delta - i\infty}^{\delta + i\infty} \frac{d\omega}{2\pi i} \left(\frac{s}{s_0}\right)^\omega G_\omega(\underline{k}, \underline{k}', \underline{r})$$

$\leftarrow$  multi-Regge kinematics



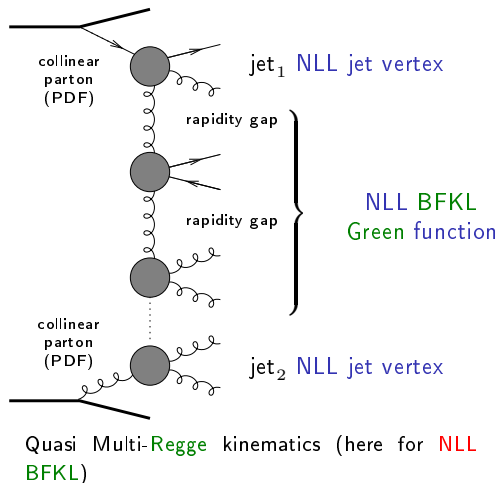
## Mueller Navelet jets at LL BFKL

- in LL BFKL ( $\sim \sum (\alpha_s \ln s)^n$ ), emission between these jets  $\rightarrow$  **strong decorrelation** between the relative azimuthal angle jets, incompatible with  $p\bar{p}$  Tevatron collider data
- a collinear treatment at next-to-leading order (NLO) can describe the data
- important issue: non-conservation of energy-momentum along the BFKL ladder. A LL BFKL-based Monte Carlo combined with e-m conservation improves dramatically the situation (Orr and Stirling)



## Mueller Navelet jets at NLL BFKL

- up to now, the subseries  $\alpha_s \sum (\alpha_s \ln s)^n$  NLL was included only in the exchanged Pomeron state, and not inside the jet vertices Sabio Vera, Schwennsen Marquet, Royon
- the common belief was that these corrections should not be important



## Angular coefficients

$$\mathcal{C}_m \equiv \int d\phi_{J1} d\phi_{J2} \cos(m(\phi_{J1} - \phi_{J2} - \pi)) \\ \times \int d^2\mathbf{k}_1 d^2\mathbf{k}_2 \Phi(\mathbf{k}_{J1}, x_{J1}, -\mathbf{k}_1) G(\mathbf{k}_1, \mathbf{k}_2, \hat{s}) \Phi(\mathbf{k}_{J2}, x_{J2}, \mathbf{k}_2).$$

- $m = 0 \implies$  cross-section

$$\frac{d\sigma}{d|\mathbf{k}_{J1}| d|\mathbf{k}_{J2}| dy_{J1} dy_{J2}} = \mathcal{C}_0$$

- $m > 0 \implies$  azimuthal decorrelation

$$\langle \cos(m\phi) \rangle \equiv \langle \cos(m(\phi_{J1} - \phi_{J2} - \pi)) \rangle = \frac{\mathcal{C}_m}{\mathcal{C}_0}$$

## Rely on LL BFKL eigenfunctions

- LL BFKL eigenfunctions:

$$E_{n,\nu}(\mathbf{k}_1) = \frac{1}{\pi\sqrt{2}} (\mathbf{k}_1^2)^{i\nu - \frac{1}{2}} e^{in\phi_1}$$

- decompose  $\Phi$  on this basis
- use the known LL eigenvalue of the BFKL equation on this basis:

$$\omega(n, \nu) = \bar{\alpha}_s \chi_0 \left( |n|, \frac{1}{2} + i\nu \right)$$

with  $\chi_0(n, \gamma) = 2\Psi(1) - \Psi\left(\gamma + \frac{n}{2}\right) - \Psi\left(1 - \gamma + \frac{n}{2}\right)$

( $\Psi(x) = \Gamma'(x)/\Gamma(x)$ ,  $\bar{\alpha}_s = N_c \alpha_s / \pi$ )

- $\implies$  master formula:

$$\mathcal{C}_m = (4 - 3\delta_{m,0}) \int d\nu C_{m,\nu}(|\mathbf{k}_{J1}|, x_{J,1}) C_{m,\nu}^*(|\mathbf{k}_{J2}|, x_{J,2}) \left( \frac{\hat{s}}{s_0} \right)^{\omega(m,\nu)}$$

with  $C_{m,\nu}(|\mathbf{k}_J|, x_J) = \int d\phi_J d^2\mathbf{k} dx f(x) V(\mathbf{k}, x) E_{m,\nu}(\mathbf{k}) \cos(m\phi_J)$

- at NLL, same master formula: just change  $\omega(m, \nu)$  and  $V$  (although  $E_{n,\nu}$  are not anymore eigenfunctions)

## NLL Green's function: rely on LL BFKL eigenfunctions

- NLL BFKL kernel is not conformal invariant
- LL  $E_{n,\nu}$  are not anymore eigenfunction
- this can be overcome by considering the eigenvalue as an operator with a part containing  $\frac{\partial}{\partial \nu}$
- it acts on the impact factor

$$\omega(n, \nu) = \bar{\alpha}_s \chi_0 \left( |n|, \frac{1}{2} + i\nu \right) + \bar{\alpha}_s^2 \left[ \chi_1 \left( |n|, \frac{1}{2} + i\nu \right) - \frac{\pi b_0}{2N_c} \chi_0 \left( |n|, \frac{1}{2} + i\nu \right) \underbrace{\left\{ -2 \ln \mu_R^2 - i \frac{\partial}{\partial \nu} \ln \frac{C_{n,\nu}(|\mathbf{k}_{J1}|, x_{J,1})}{C_{n,\nu}(|\mathbf{k}_{J2}|, x_{J,2})} \right\}}_{2 \ln \frac{|\mathbf{k}_{J1}| \cdot |\mathbf{k}_{J2}|}{\mu_R^2}} \right],$$



## Collinear improved Green's function at NLL

- one may improve the NLL **BFKL** kernel for  $n = 0$  by imposing its compatibility with **DGLAP** in the collinear limit  
Salam; Ciafaloni, Colferai
- usual (anti)collinear poles in  $\gamma = 1/2 + i\nu$  (resp.  $1 - \gamma$ ) are shifted by  $\omega/2$
- one practical implementation:
  - the new kernel  $\bar{\alpha}_s \chi^{(1)}(\gamma, \omega)$  with shifted poles replaces

$$\bar{\alpha}_s \chi_0(\gamma, 0) + \bar{\alpha}_s^2 \chi_1(\gamma, 0)$$

- $\omega(0, \nu)$  is obtained by solving the implicit equation

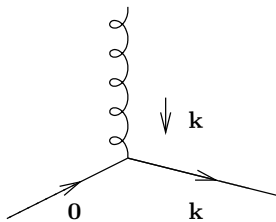
$$\omega(0, \nu) = \bar{\alpha}_s \chi^{(1)}(\gamma, \omega(0, \nu))$$

for  $\omega(n, \nu)$  numerically.

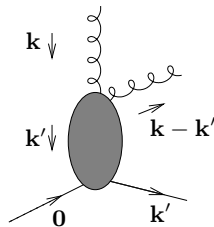
- there is no need for any jet vertex improvement because of the absence of  $\gamma$  and  $1 - \gamma$  poles (numerical proof using **Cauchy** theorem "backward")

$\mathbf{k}, \mathbf{k}' =$  Euclidian two dimensional vectors

LL jet vertex:



NLL jet vertex:



$$V_a^{(0)}(\mathbf{k}, x) = h_a^{(0)}(\mathbf{k}) \mathcal{S}_J^{(2)}(\mathbf{k}; x)$$

$$\text{with: } h_a^{(0)}(\mathbf{k}) = \frac{\alpha_s}{\sqrt{2}} \frac{C_{A/F}}{\mathbf{k}^2},$$

$$\mathcal{S}_J^{(2)}(\mathbf{k}; x) = \delta\left(1 - \frac{x_J}{x}\right) |\mathbf{k}_J| \delta^{(2)}(\mathbf{k} - \mathbf{k}_J)$$

$$\begin{aligned}
 V_q^{(1)}(\mathbf{k}, x) = & \left[ \left( \frac{3}{2} \ln \frac{\mathbf{k}^2}{\Lambda^2} - \frac{15}{4} \right) \frac{C_F}{\pi} + \left( \frac{85}{36} + \frac{\pi^2}{4} \right) \frac{C_A}{\pi} - \frac{5}{18} \frac{N_f}{\pi} - b_0 \ln \frac{\mathbf{k}^2}{\mu^2} \right] V_q^{(0)}(\mathbf{k}, x) \\
 & + \int dz \left( \frac{C_F}{\pi} \frac{1-z}{2} + \frac{C_A}{\pi} \frac{z}{2} \right) V_q^{(0)}(\mathbf{k}, xz) \\
 & + \frac{C_A}{\pi} \int \frac{d^2 \mathbf{k}'}{\pi} \int dz \left[ \frac{1+(1-z)^2}{2z} \left( (1-z) \frac{(\mathbf{k}-\mathbf{k}') \cdot ((1-z)\mathbf{k}-\mathbf{k}')}{(\mathbf{k}-\mathbf{k}')^2 ((1-z)\mathbf{k}-\mathbf{k}')^2} h_q^{(0)}(\mathbf{k}') S_J^{(3)}(\mathbf{k}', \mathbf{k}-\mathbf{k}', xz; x) \right. \right. \\
 & \quad \left. \left. - \frac{1}{\mathbf{k}'^2} \Theta(\Lambda^2 - \mathbf{k}'^2) V_q^{(0)}(\mathbf{k}, xz) \right) \right. \\
 & \quad \left. - \frac{1}{z(\mathbf{k}-\mathbf{k}')^2} \Theta(|\mathbf{k}-\mathbf{k}'| - z(|\mathbf{k}-\mathbf{k}'| + |\mathbf{k}'|)) V_q^{(0)}(\mathbf{k}', x) \right] \\
 & + \frac{C_F}{2\pi} \int dz \frac{1+z^2}{1-z} \int \frac{d^2 \mathbf{l}}{\pi \mathbf{l}^2} \left[ \frac{\mathcal{N} C_F}{\mathbf{l}^2 + (1-\mathbf{k})^2} (S_J^{(3)}(z\mathbf{k} + (1-z)\mathbf{l}, (1-z)(\mathbf{k}-\mathbf{l}), x(1-z); x) \right. \\
 & \quad \left. + S_J^{(3)}(\mathbf{k} - (1-z)\mathbf{l}, (1-z)\mathbf{l}, x(1-z); x) \right. \\
 & \quad \left. - \Theta \left( \frac{\Lambda^2}{(1-z)^2} - \mathbf{l}^2 \right) \left( V_q^{(0)}(\mathbf{k}, x) + V_q^{(0)}(\mathbf{k}, xz) \right) \right] \\
 & - \frac{2C_F}{\pi} \int dz \left( \frac{1}{1-z} \right) \int \frac{d^2 \mathbf{l}}{\pi \mathbf{l}^2} \left[ \frac{\mathcal{N} C_F}{\mathbf{l}^2 + (1-\mathbf{k})^2} S_J^{(2)}(\mathbf{k}, x) - \Theta \left( \frac{\Lambda^2}{(1-z)^2} - \mathbf{l}^2 \right) V_q^{(0)}(\mathbf{k}, x) \right]
 \end{aligned}$$

$$\begin{aligned}
 V_g^{(1)}(\mathbf{k}, x) = & \left[ \left( \frac{11}{6} \frac{C_A}{\pi} - \frac{1}{3} \frac{N_f}{\pi} \right) \ln \frac{\mathbf{k}^2}{\Lambda^2} + \left( \frac{\pi^2}{4} - \frac{67}{36} \right) \frac{C_A}{\pi} + \frac{13}{36} \frac{N_f}{\pi} - b_0 \ln \frac{\mathbf{k}^2}{\mu^2} \right] V_g^{(0)}(\mathbf{k}, x) \\
 & + \int dz \frac{N_f}{\pi} \frac{C_F}{C_A} z(1-z) V_g^{(0)}(\mathbf{k}, xz) \\
 & + \frac{N_f}{\pi} \int \frac{d^2 \mathbf{k}'}{\pi} \int_0^1 dz P_{qg}(z) \left[ \frac{h_q^{(0)}(\mathbf{k}')}{(\mathbf{k} - \mathbf{k}')^2 + \mathbf{k}'^2} S_J^{(3)}(\mathbf{k}', \mathbf{k} - \mathbf{k}', xz; x) - \frac{1}{\mathbf{k}'^2} \Theta(\Lambda^2 - \mathbf{k}'^2) V_q^{(0)}(\mathbf{k}, xz) \right] \\
 & + \frac{N_f}{2\pi} \int \frac{d^2 \mathbf{k}'}{\pi} \int_0^1 dz P_{qg}(z) \frac{\mathcal{N}C_A}{((1-z)\mathbf{k} - \mathbf{k}')^2} \left[ z(1-z) \frac{(\mathbf{k} - \mathbf{k}') \cdot \mathbf{k}'}{(\mathbf{k} - \mathbf{k}')^2 \mathbf{k}'^2} S_J^{(3)}(\mathbf{k}', \mathbf{k} - \mathbf{k}', xz; x) \right. \\
 & \quad \left. - \frac{1}{\mathbf{k}^2} \Theta(\Lambda^2 - ((1-z)\mathbf{k} - \mathbf{k}')^2) S_J^{(2)}(\mathbf{k}, x) \right] \\
 & + \frac{C_A}{\pi} \int_0^1 \frac{dz}{1-z} [(1-z)P(1-z)] \int \frac{d^2 \mathbf{l}}{\pi \mathbf{l}^2} \left\{ \frac{\mathcal{N}C_A}{\mathbf{l}^2 + (1-\mathbf{k})^2} [S_J^{(3)}(z\mathbf{k} + (1-z)\mathbf{l}, (1-z)(\mathbf{k} - \mathbf{l}), x(1-z); x) \right. \\
 & \quad \left. + S_J^{(3)}(\mathbf{k} - (1-z)\mathbf{l}, (1-z)\mathbf{l}, x(1-z); x)] \right. \\
 & \quad \left. - \Theta \left( \frac{\Lambda^2}{(1-z)^2} - \mathbf{l}^2 \right) [V_g^{(0)}(\mathbf{k}, x) + V_g^{(0)}(\mathbf{k}, xz)] \right\} \\
 & - \frac{2C_A}{\pi} \int_0^1 \frac{dz}{1-z} \int \frac{d^2 \mathbf{l}}{\pi \mathbf{l}^2} \left[ \frac{\mathcal{N}C_A}{\mathbf{l}^2 + (1-\mathbf{k})^2} S_J^{(2)}(\mathbf{k}, x) - \Theta \left( \frac{\Lambda^2}{(1-z)^2} - \mathbf{l}^2 \right) V_g^{(0)}(\mathbf{k}, x) \right] \\
 & + \frac{C_A}{\pi} \int \frac{d^2 \mathbf{k}'}{\pi} \int_0^1 dz \left[ P(z) \left( (1-z) \frac{(\mathbf{k} - \mathbf{k}') \cdot ((1-z)\mathbf{k} - \mathbf{k}')}{(\mathbf{k} - \mathbf{k}')^2 ((1-z)\mathbf{k} - \mathbf{k}')^2} h_g^{(0)}(\mathbf{k}') \right. \right. \\
 & \quad \left. \left. \times S_J^{(3)}(\mathbf{k}', \mathbf{k} - \mathbf{k}', xz; x) - \frac{1}{\mathbf{k}'^2} \Theta(\Lambda^2 - \mathbf{k}'^2) V_g^{(0)}(\mathbf{k}, xz) \right) \right. \\
 & \quad \left. - \frac{1}{z(\mathbf{k} - \mathbf{k}')^2} \Theta(|\mathbf{k} - \mathbf{k}'| - z(|\mathbf{k} - \mathbf{k}'| + |\mathbf{k}'|)) V_g^{(0)}(\mathbf{k}', x) \right]
 \end{aligned}$$

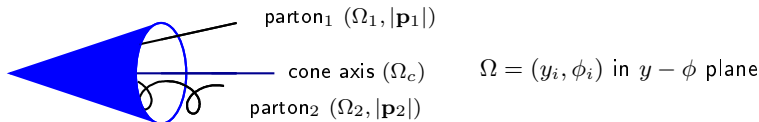
## Jet algorithms

- a jet algorithm should be IR safe, both for soft and collinear singularities
- the most common jet algorithm are:
  - $k_t$  algorithms (IR safe but time consuming for multiple jets configurations)
  - cone algorithm (not IR safe in general; can be made IR safe at NLO: Ellis, Kunszt, Soper)

## Cone jet algorithm at NLO (Ellis, Kunszt, Soper)

- Should partons  $(|\mathbf{p}_1|, \phi_1, y_1)$  and  $(|\mathbf{p}_2|, \phi_2, y_2)$  be combined in a single jet?  
 $|\mathbf{p}_i|$  = transverse energy deposit in the calorimeter cell  $i$  of parameter  $\Omega = (y_i, \phi_i)$  in  $y - \phi$  plane
- define transverse energy of the jet:  $p_J = |\mathbf{p}_1| + |\mathbf{p}_2|$
- jet axis:

$$\Omega_c \begin{cases} y_J = \frac{|\mathbf{p}_1| y_1 + |\mathbf{p}_2| y_2}{p_J} \\ \phi_J = \frac{|\mathbf{p}_1| \phi_1 + |\mathbf{p}_2| \phi_2}{p_J} \end{cases}$$



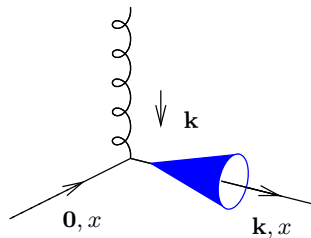
If distances  $|\Omega_i - \Omega_c|^2 \equiv (y_i - y_c)^2 + (\phi_i - \phi_c)^2 < R^2$  ( $i = 1$  and  $i = 2$ )

$\implies$  partons 1 and 2 are in the same cone  $\Omega_c$

combined condition:  $|\Omega_1 - \Omega_2| < \frac{|\mathbf{p}_1| + |\mathbf{p}_2|}{\max(|\mathbf{p}_1|, |\mathbf{p}_2|)} R$

## LL jet vertex and cone algorithm

$\mathbf{k}, \mathbf{k}' =$  Euclidian two dimensional vectors



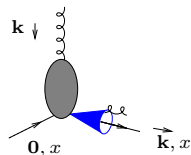
$$\mathcal{S}_J^{(2)}(k_{\perp}; x) = \delta\left(1 - \frac{x_J}{x}\right) |\mathbf{k}| \delta^{(2)}(\mathbf{k} - \mathbf{k}_J)$$



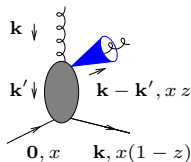
## NLL jet vertex and cone algorithm

$\mathbf{k}, \mathbf{k}' =$  Euclidian two dimensional vectors

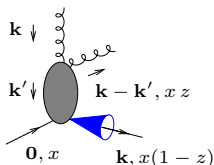
$$\mathcal{S}_J^{(3,\text{cone})}(\mathbf{k}', \mathbf{k} - \mathbf{k}', xz; x) =$$



$$\mathcal{S}_J^{(2)}(\mathbf{k}, x) \Theta \left( \left[ \frac{|\mathbf{k} - \mathbf{k}'| + |\mathbf{k}'|}{\max(|\mathbf{k} - \mathbf{k}'|, |\mathbf{k}'|)} R_{\text{cone}} \right]^2 - [\Delta y^2 + \Delta \phi^2] \right)$$



$$+ \mathcal{S}_J^{(2)}(\mathbf{k} - \mathbf{k}', xz) \Theta \left( [\Delta y^2 + \Delta \phi^2] - \left[ \frac{|\mathbf{k} - \mathbf{k}'| + |\mathbf{k}'|}{\max(|\mathbf{k} - \mathbf{k}'|, |\mathbf{k}'|)} R_{\text{cone}} \right]^2 \right)$$



$$+ \mathcal{S}_J^{(2)}(\mathbf{k}', x(1-z)) \Theta \left( [\Delta y^2 + \Delta \phi^2] - \left[ \frac{|\mathbf{k} - \mathbf{k}'| + |\mathbf{k}'|}{\max(|\mathbf{k} - \mathbf{k}'|, |\mathbf{k}'|)} R_{\text{cone}} \right]^2 \right),$$

Using a IR safe jet algorithm, Mueller-Navelet jets at NLL are finite

- UV sector:
  - the NLL impact factor contains UV divergencies  $1/\epsilon$
  - they are absorbed by the renormalization of the coupling:  $\alpha_S \rightarrow \alpha_S(\mu_R)$
- IR sector:
  - PDF have IR collinear singularities: pole  $1/\epsilon$  at LO
  - these collinear singularities can be compensated by collinear singularities of the two jets vertices and the real part of the BFKL kernel
  - the remaining collinear singularities compensate exactly among themselves
  - soft singularities of the real and virtual BFKL kernel, and of the jets vertices compensates among themselves

This was shown for both quark and gluon initiated vertices (Bartels, Colferai, Vacca)

- one sums up  $\sum (\alpha_s \ln \hat{s}/s_0)^n + \alpha_s \sum (\alpha_s \ln \hat{s}/s_0)^n$  ( $\hat{s} = x_1 x_2 s$ )
- at LL  $s_0$  is arbitrary
- natural choice:  $s_{0,i} = \sqrt{s_{0,1} s_{0,2}}$   $s_{0,i}$  for each of the scattering objects
  - possible choice:  $s_{0,i} = (|\mathbf{k}_J| + |\mathbf{k}_J - \mathbf{k}|)^2$  (Bartels, Colferai, Vacca)
    - but depend on  $\mathbf{k}$ , which is integrated over
    - $\hat{s}$  is not an external scale ( $x_{1,2}$  are integrated over)
  - we prefer

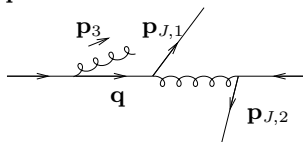
$$\left. \begin{aligned}
 s_{0,1} &= (|\mathbf{k}_{J1}| + |\mathbf{k}_{J1} - \mathbf{k}_1|)^2 \rightarrow s'_{0,1} = \frac{x_1^2}{x_{J,1}^2} \mathbf{k}_{J1}^2 \\
 s_{0,2} &= (|\mathbf{k}_{J2}| + |\mathbf{k}_{J2} - \mathbf{k}_2|)^2 \rightarrow s'_{0,2} = \frac{x_2^2}{x_{J,2}^2} \mathbf{k}_{J2}^2
 \end{aligned} \right\} \frac{\hat{s}}{s_0} \rightarrow \frac{\hat{s}}{s'_0} = \frac{x_{J,1} x_{J,2} s}{|\mathbf{k}_{J1}| |\mathbf{k}_{J2}|} = e^{y_{J,1} - y_{J,2}} \equiv e^Y$$

- $s_0 \rightarrow s'_0$  affects
  - the BFKL NLL Green function
  - the impact factors:

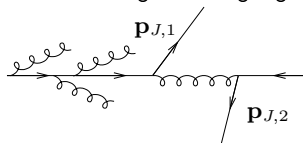
$$\Phi_{\text{NLL}}(\mathbf{k}_i; s'_{0,i}) = \Phi_{\text{NLL}}(\mathbf{k}_i; s_{0,i}) + \int d^2\mathbf{k}' \Phi_{\text{LL}}(\mathbf{k}'_i) \mathcal{K}_{\text{LL}}(\mathbf{k}'_i, \mathbf{k}_i) \frac{1}{2} \ln \frac{s'_{0,i}}{s_{0,i}} \quad (1)$$

- numerical stability (non azimuthal averaging of LL subtraction) improved with the choice  $s_{0,i} = (\mathbf{k}_i - 2\mathbf{k}_{Ji})^2$  (then replaced by  $s'_{0,i}$  after numerical integration)
- (1) can be used to test  $s_0 \rightarrow \lambda s_0$  dependence

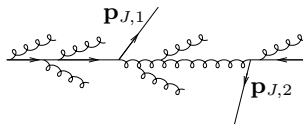
- Initial state radiation (unseen) produces divergencies if one touches the collinear singularity  $\mathbf{q}^2 \rightarrow 0$



- they are compensated by virtual corrections
- this compensation is in practice difficult to implement when for some reason this additional emission is in a "corner" of the phase space (dip in the differential cross-section)
- this is the case when  $\mathbf{p}_1 + \mathbf{p}_2 \rightarrow 0$
- this calls for a resummation of large remaining logs  $\Rightarrow$  **Sudakov** resummation



- since these resummation have never been investigated in this context, one should better avoid that region
- note that for **BFKL**, due to additional emission between the two jets, one may expect a less severe problem (at least a smearing in the dip region  $|\mathbf{p}_1| \sim |\mathbf{p}_2|$ )



- this may however not mean that the region  $|\mathbf{p}_1| \sim |\mathbf{p}_2|$  is perfectly trustable even in a **BFKL** type of treatment
- we now investigate a region where NLL **DGLAP** is under control